ISSN 1674-1056
http://cpb.iphy.ac.cn
http://iopscience.iop.org/cpb
中国物理 B
Chinese Physics
中国物理
Chinese Physics B

Regulating element distribution to improve magnetic properties of sintered Nd-Fe-B/Tb-Fe-B composite magnets

Zhu-Bai Li(李柱柏), Jing-Yan Zuo(左敬燕), Dong-Shan Wang(王东山), Fei Liu(刘飞), Xue-Feng Zhang(张雪峰)

Citation: Chin. Phys. B . 2019, 28(7): 077503. **doi:** 10.1088/1674-1056/28/7/077503
Journal homepage: http://cpb.iphy.ac.cn; http://iopscience.iop.org/cpb

What follows is a list of articles you may be interested in

Micromagnetic simulations of reversal magnetization in cerium-containing magnets

Lei Li(李磊), Shengzhi Dong(董生智), Hongsheng Chen(陈红升), Ruijiao Jiang(姜瑞姣), Dong Li(李栋), Rui Han(韩瑞), Dong Zhou(周栋), Minggang Zhu(朱明刚), Wei Li(李卫), Wei Sun(孙威)
Chin. Phys. B . 2019, 28(3): 037502. **doi:** 10.1088/1674-1056/28/3/037502

Rare earth permanent magnets prepared by hot deformation process

Ren-Jie Chen(陈仁杰), Ze-Xuan Wang(王泽轩), Xu Tang(唐旭), Wen-Zong Yin(尹文宗), Chao-Xiang Jin(靳朝相), Jin-Yun Ju(剧锦云), Don Lee(李东), A-Ru Yan(闫阿儒)
Chin. Phys. B . 2018, 27(11): 117504. **doi:** 10.1088/1674-1056/27/11/117504

Mn-based permanent magnets

Jinbo Yang(杨金波), Wenyun Yang(杨文云), Zhuyin Shao(邵珠印), Dong Liang(梁栋), Hui Zhao(赵辉), Yuanhua Xia(夏元华), Yunbo Yang(杨云波)
Chin. Phys. B . 2018, 27(11): 117503. **doi:** 10.1088/1674-1056/27/11/117503

Nanocrystalline and nanocomposite permanent magnets by melt spinning technique

Chuanbing Rong(荣传兵), Baogen Shen(沈保根)
Chin. Phys. B . 2018, 27(11): 117502. **doi:** 10.1088/1674-1056/27/11/117502

Micromagnetism simulation on effects of soft phase size on $Nd_2Fe_{14}B/\alpha$–Fe nanocomposite magnet with soft phase imbedded in hard phase

Yu-Qing Li(李玉卿), Ming Yue(岳明), Yi Peng(彭懿), Hong-Guo Zhang(张红国)
Chin. Phys. B . 2018, 27(8): 087502. **doi:** 10.1088/1674-1056/27/8/087502

Regulating element distribution to improve magnetic properties of sintered Nd–Fe–B/Tb–Fe–B composite magnets*

Zhu-Bai Li(李柱柏)[1,2,†], Jing-Yan Zuo(左敬燕)[1], Dong-Shan Wang(王东山)[2], Fei Liu(刘飞)[1,2], and Xue-Feng Zhang(张雪峰)[1,2]

[1] *Key Laboratory of Integrated Exploitation of Bayan Obo Multi-Metal Resources, Inner Mongolia University of Science and Technology, Baotou* 014010, *China*

[2] *School of Science, Inner Mongolia University of Science and Technology, Baotou* 014010, *China*

(Received 13 January 2019; revised manuscript received 6 May 2019; published online 12 June 2019)

Nd content was varied in $Nd_{13.2-x}Fe_{80.8+x}B_6$ ($x = 0$, 0.5, 1, and 1.5) to optimize the magnetic properties of sintered Nd–Fe–B/Tb–Fe–B composite magnets, which were prepared by mixing 9 g of Nd–Fe–B with 1 g of $Tb_{17}Fe_{75}B_8$ powder. In conventional magnets, by reducing Nd content, the coercivity of 10.4 kOe in $Nd_{13.2}Fe_{80.8}B_6$ decreases to 7.2 kOe in $Nd_{12.2}Fe_{81.8}B_6$; meanwhile, in Nd–Fe–B/Tb–Fe–B magnets the coercivity does not decrease when reducing Nd content. In the intergranular phase, the Tb content increases owing to the reducing Nd content of the Nd–Fe–B alloy in the sintered composite magnets. Therefore, the excess Tb in $Tb_{17}Fe_{75}B_8$ enters the intergranular phase, and more Tb atoms can substitute for Nd at the grain boundary of the Nd–Fe–B phase, leading to a more significant increase in coercivity. The remanence increases with reducing Nd content, and the energy product of 39.1 MGOe with a high coercivity of 21.0 kOe is obtained in $Nd_{12.2}Fe_{81.8}B_6/Tb_{17}Fe_{75}B_8$ magnets. These investigations show that magnetic properties can be further improved by regulating the element distribution in sintered composite magnets.

Keywords: composite magnets, coercivity, intergranular phase, element distribution

PACS: 75.50.Vv, 75.50.Ww, 75.60.Ej **DOI:** 10.1088/1674-1056/28/7/077503

1. Introduction

Nd–Fe–B magnets are essential components in many technology fields owing to their high energy product,[1–3] but their coercivity is relatively low and far less than the theoretical value.[4] For meeting the technology demand of hybrid/electric vehicles, it is necessary to improve the coercivity and thermal stability of Nd–Fe–B-based magnets. The grain boundary diffusion of Dy/Tb alloys could significantly improve the coercivity;[5–8] however, this is only suitable for small magnets. Recently, it was found that the coercivity could be enhanced and the behaviors of magnetization reversal are uniform in resource-saving magnets with dual main phases.[9–14] The coercivity also increases in sintered magnets prepared by the addition of Tb–Fe–B powders to Nd–Fe–B,[15] and the increase has a nearly linear relationship with the added amount of Tb–Fe–B. This effect is better than that of conventional dual-alloy methods, in which the coercivity increases very slowly and even decreases for a large amount of DyH_x added to Nd–Fe–B powders.[16] Both the ultrahigh magnetocrystalline anisotropy of the $Tb_2Fe_{14}B$ phase and Tb atomic diffusion possibly contribute to the improvement of coercivity.[15] It is noted that Nd atoms also diffuse via the intergranular phase during high-temperature sintering, and therefore Nd would substitute for Tb in the $Tb_2Fe_{14}B$ phase, thus reducing its magnetocrystalline anisotropy. Provided that the diffusion of Nd could be suppressed and more Tb atoms substitute for Nd at the Nd–Fe–B grain boundary, as well as the ultrahigh magnetocrystalline anisotropy remaining in the Tb–Fe–B main phase, the coercivity may increase more greatly. In this paper, the content of Nd of the Nd–Fe–B alloy was varied, and the Tb content was increased in the Tb–Fe–B alloy. These are expected to regulate the element distribution for optimizing the magnetic properties in sintered Nd–Fe–B/Tb–Fe–B magnets.

2. Experiment

$Nd_{13.2-x}Fe_{80.8+x}B_6$ ($x = 0$, 0.5, 1, and 1.5) powders, in which the content of Nd was reduced from 13.2 at.% to 11.7 at.%, were prepared by the induction melting of Nd, Fe, and Fe–B alloys, followed by hydrogen decrepitation and jet-milling. $Tb_{17}Fe_{75}B_8$ powders were prepared through induction melting, hydrogen decrepitation, and ball-milling, and the Tb atomic percent, 17 at.%, was much higher than the Tb stoichiometry of 11.7 at.% in $Tb_2Fe_{14}B$. Nine grams of Nd–Fe–B powder was mixed with 1 g of $Tb_{17}Fe_{75}B_8$ powder, and then blended for 10 min to ensure compositional uniformity. Nd–Fe–B powder and the mixture of Nd–Fe–B/Tb–Fe–B (mass ratio of 9 : 1) were compressed, separately, after alignment under a 2 T pulsed magnetic field. The compacts were sintered in a vacuum at 1050–1060 ℃ for 2 h, followed by anneal-

*Project supported by the National Natural Science Foundation of China (Grant Nos. 51861030 and 51571126) and the National Key Research and Development Program of China (Grant No. 2016YFB0700900).

†Corresponding author. E-mail: lzbgj@163.com

© 2019 Chinese Physical Society and IOP Publishing Ltd

ing at 510 ℃ for 2 h. The demagnetization curves were measured using an NIM-200 C loop tracer. X-ray diffraction measurement was performed using Co $K\alpha$ radiation to check the phase constitution. The microstructure and chemical composition were observed by a scanning electron microscope (SEM) with backscattered electrons (BSE) and an energy dispersive spectrometer (EDS), respectively.

3. Results and discussion

X-ray diffraction patterns confirm that all of the samples contain the $R_2Fe_{14}B$ main phase (shown in Fig. 1), and the unidentified phase should be the intergranular phase.[17] There is a small amount of α-Fe phases in $Nd_{11.7}Fe_{82.3}B_6$, and the rather low content of Nd and high content of Fe are ascribed to the existence of the minor phase of α-Fe. Figure 2 shows the surface micromorphology of the magnets observed by SEM with BSE. The brighter regions correspond to the intergranular phase, and the dark regions correspond to the main phase of $R_2Fe_{14}B$. The size of some intergranular phases is larger in the magnets with the higher Nd content, and the amount of intergranular phases decreases with the reduction in Nd content. The element distribution was inspected by EDS (shown in Fig. 3). The left panel is Nd mapping, and the right is Tb mapping. The color is brighter in regions with a high content of the corresponding element. In Nd mapping, the intergranular phase is brighter, which is consistent with the micromorphology presented in Fig. 2, thus confirming the Nd-rich characteristics of the intergranular phase. The darker regions labeled by the dotted boxes are Nd-lean regions, and these regions are brighter in the Tb mapping, thus indicating that the magnets consist of Tb-rich main phases of $R_2Fe_{14}B$. The area with the most Tb-rich main phases decreases with reducing Nd content. With the reduction in Nd content, the regions of the intergranular phase become a little brighter, implying an increase in Tb content in the intergranular phase.

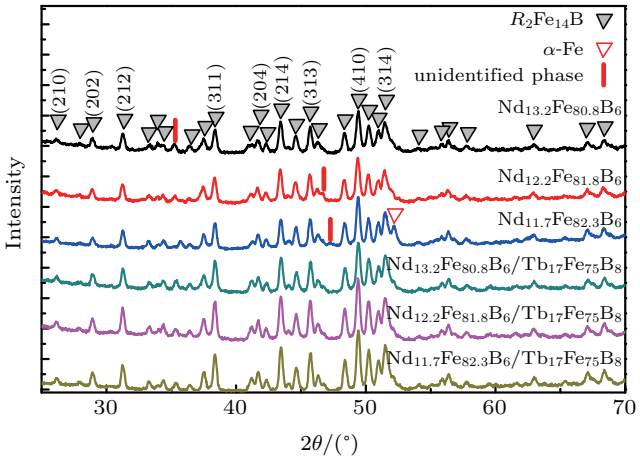


Fig. 1. XRD patterns using Co $K\alpha$ radiation for the sintered magnets of Nd–Fe–B and Nd–Fe–B/Tb–Fe–B.

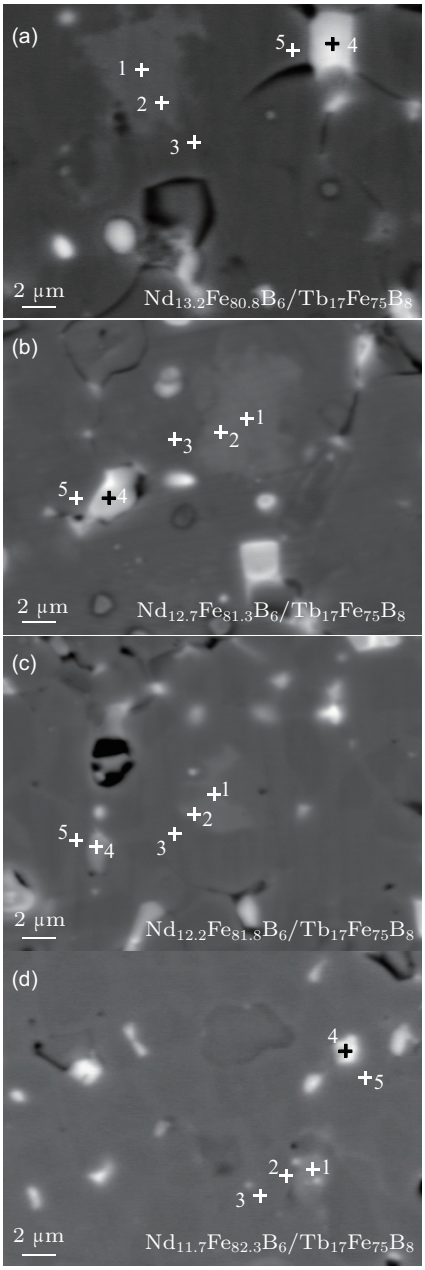


Fig. 2. The surface micromorphology of the sintered magnets of (a) $Nd_{13.2}Fe_{80.8}B_6/Tb_{17}Fe_{75}B_8$, (b) $Nd_{12.7}Fe_{81.3}B_6/Tb_{17}Fe_{75}B_8$, (c) $Nd_{12.2}Fe_{81.8}B_6/Tb_{17}Fe_{75}B_8$, and (d) $Nd_{11.7}Fe_{82.3}B_6/Tb_{17}Fe_{75}B_8$.

The element contents were checked by EDS in the dual-main-phase magnets. In Figs. 2 and 3, spots 1–3 are in the main phase, and spot 4 is in the intergranular phase, near which is spot 5 in the Nd-rich main phase. The contents of Nd, Tb, and Fe are listed in Table 1. In Fig. 3(a), the content of Tb is 10.67 at.% for spot 1, less than 13.2 at.% in the master alloy, and the content of Nd is 2.23 at.%. For spot 3, the content of Tb is 2.28 at.% in the Nd-rich main phase. Although there are two main phases in the magnets, the chemical compositions are very different from those of the master alloy due to the atomic interdiffusion.[18] In the intergranular phase, the atomic ratio of Tb and Nd is 2.86 : 44.77 for spot 4 (shown in Fig. 3(a)), and that increases to 4.02 : 38.52 for the magnets with a Nd content of 12.2 at.% (shown in Fig. 3(d)). This fact

verifies the increase in Tb content and the decrease in Nd content in the intergranular phase when reducing the Nd content of Nd–Fe–B.

Table 1. The atomic percents of elements for spots 1–5 shown in Fig. 3.

		1	2	3	4	5
3(a)	O				20.42	
	Fe	87.10	87.26	87.33	31.95	86.98
	Nd	2.23	6.83	10.39	44.77	11.45
	Tb	10.67	5.91	2.28	2.86	1.57
3(b)	O				20.17	
	Fe	87.46	86.98	87.23	45.82	86.98
	Nd	1.24	6.94	10.84	32.20	11.96
	Tb	11.30	6.08	1.93	1.81	1.06
3(c)	O				49.29	
	Fe	86.96	87.12	86.63	8.35	87.06
	Nd	4.54	7.49	10.22	38.41	11.71
	Tb	8.50	5.39	3.15	3.95	1.23
3(d)	O				45.16	
	Fe	87.27	87.31	87.33	12.30	87.33
	Nd	2.46	10.45	11.69	38.52	10.69
	Tb	10.27	2.24	0.98	4.02	1.98

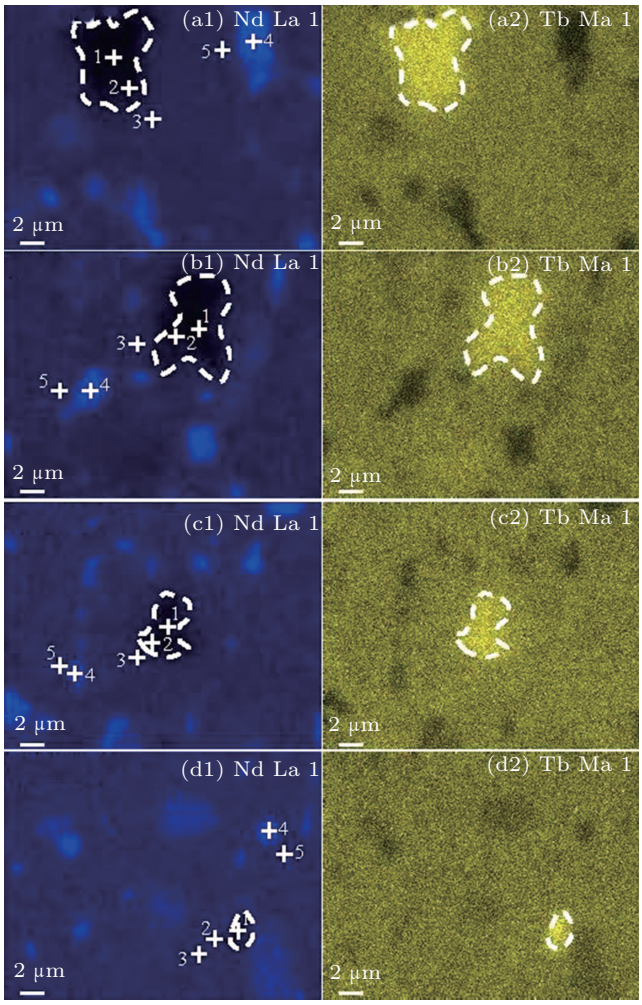


Fig. 3. Element mappings of Nd and Tb for magnets of (a) $Nd_{13.2}Fe_{80.8}B_6/Tb_{17}Fe_{75}B_8$, (b) $Nd_{12.7}Fe_{81.3}B_6/Tb_{17}Fe_{75}B_8$, (c) $Nd_{12.2}Fe_{81.8}B_6/Tb_{17}Fe_{75}B_8$, and (d) $Nd_{11.7}Fe_{82.3}B_6/Tb_{17}Fe_{75}B_8$.

The change in element distributions of Tb and Nd may affect the magnetic properties of the composite magnets. Figure 4 shows the demagnetization curves of all samples, and the magnetic properties are listed in Table 2. For the $Nd_{13.2}Fe_{80.8}B_6$ magnet, the coercivity is 10.4 kOe. With the reduction in Nd content, the coercivity decreases (to 7.2 kOe in $Nd_{12.2}Fe_{81.8}B_6$). The magnetic properties deteriorate for $Nd_{11.7}Fe_{82.3}B_6$. The decrease in coercivity may result from the increase in defects at the grain boundary due to the reduction in rare-earth content; furthermore, due to the weak magnetic properties and the dipolar interaction, there is no demagnetization curve in the second quadrant for $Nd_{11.7}Fe_{82.3}B_6$.[19] In the Nd–Fe–B/Tb–Fe–B composite magnets, the coercivities are 21.7 kOe, 21.8 kOe, 21.0 kOe, and 21.8 kOe, respectively, for Nd contents of 13.2 at.%, 12.7 at.%, 12.2 at.%, and 11.7 at.%. The addition of 1 g of $Tb_{17}Fe_{75}B_8$ powder to 9 g of Nd–Fe–B powder leads to a large increase in coercivity. It is noted that unlike the effect in the conventional sintered Nd–Fe–B magnets, the reduction in Nd content does not result in a decrease in coercivity in the Nd–Fe–B/Tb–Fe–B composite magnets.

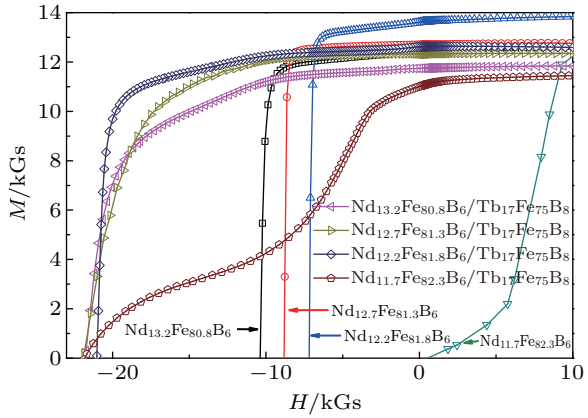


Fig. 4. The demagnetization curves for the sintered Nd–Fe–B and Nd–Fe–B/Tb–Fe–B magnets.

Table 2. Magnetic properties of the sintered magnets at room temperature.

Composition	M_r/Gs	H_c/kOe	$(BH)_{max}$/MGOe
$Nd_{13.2}Fe_{80.8}B_6$	12.4	10.4	34.6
$Nd_{12.7}Fe_{81.3}B_6$	12.7	8.9	39.9
$Nd_{12.2}Fe_{81.8}B_6$	13.6	7.2	43.0
$Nd_{11.7}Fe_{82.3}B_6$	–	–	–
$Nd_{13.2}Fe_{80.8}B_6/Tb_{17}Fe_{75}B_8$	11.7	21.7	33.6
$Nd_{12.7}Fe_{81.3}B_6/Tb_{17}Fe_{75}B_8$	12.3	21.8	37.2
$Nd_{12.2}Fe_{81.8}B_6/Tb_{17}Fe_{75}B_8$	12.6	21.0	39.1
$Nd_{11.7}Fe_{82.3}B_6/Tb_{17}Fe_{75}B_8$	11.0	21.8	21.9

During the high-temperature sintering, the main phase of $R_2Fe_{14}B$ is in the solid phase, and the intergranular phase is in the liquid phase due to its low melting point, which is the main path for atomic diffusion. For decreasing Nd content of Nd–Fe–B, the amount of free Nd atoms decreases, giving rise to an increase in the active energy for Nd diffusion.

Therefore, Nd atomic diffusion is weakened, and the excess Tb atoms in $Tb_{17}Fe_{75}B_8$ diffuse into the intergranular liquid phase. The increase in Tb content in the intergranular phase would promote the substitution for Nd at the grain boundary to form the $(Nd,Tb)_2Fe_{14}B$ phase,[20] leading to an increase in the magnetocrystalline anisotropy at the grain outer-layer; therefore, the nucleation of the reversed domain is improved in the sintered magnets.[21] This may be the main reason why the coercivity is significantly more enhanced in the sintered Nd–Fe–B/Tb–Fe–B magnets for reducing Nd content. For a rather low Nd content in $Nd_{11.7}Fe_{82.3}B_6/Tb_{17}Fe_{75}B_8$, the squareness of the demagnetization curve decreases. With the reduction in Nd content from 13.2 at.% to 12.2 at.%, both the remanence and the maximum energy product increase. The increase in remanence should result from the enhanced saturation magnetization due to the increase in Fe content in the alloys with low Nd. Furthermore, the energy product of 39.1 MGOe is the largest in $Nd_{12.2}Fe_{81.8}B_6/Tb_{17}Fe_{75}B_8$ magnets with a coercivity of 21.0 kOe. The increase in coercivity of 13.8 kOe in $Nd_{12.2}Fe_{81.8}B_6/Tb_{17}Fe_{75}B_8$ (Tb content of about 1.5 at%) is much larger than the increase of 4.1 kOe in conventional $R_{13.5}Tb_{1.5}Fe_{78}B_7$ magnets prepared by adding 1.5 at% Tb directly into Nd–Fe–B;[22] it is also larger than the increase of 8.2 kOe for 4 wt.% Tb addition in (Nd,Pr)–Fe–B.[23] As nanocomposite magnets,[24] the sintered dual-main-phase magnets bear better magnetic properties than the conventional sintered (Nd,Tb)–Fe–B magnets.

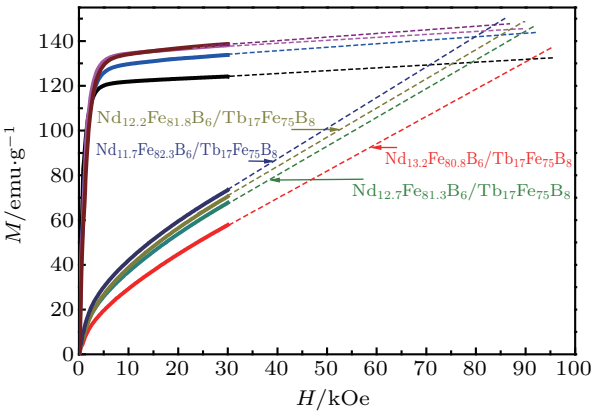


Fig. 5. The magnetization curves in the directions of easy and hard magnetization axes, and the linear extension of the experimental data up to the intersection.

The coercivity originates from the magnetocrystalline anisotropy in $R_2Fe_{14}B$ permanent magnets. Figure 5 shows the magnetization curves measured along the hard and easy magnetization axes, respectively, for these sintered Nd–Fe–B/Tb–Fe–B magnets. The magnetocrystalline anisotropy could be obtained by the intersection of the extension lines of experimental data;[25] they are 91.1 kOe, 89.2 kOe, 87.3 kOe, and 83.9 kOe, respectively, for the magnets with Nd contents of 13.2 at.%, 12.7% at.%, 12.2% at.%, and 11.7% at.%. The anisotropy field should be the average value, since the microstructure is inhomogeneous and the magnetic properties are different in different regions in the sintered magnets. Although the average anisotropy decreases with the reduction in Nd content, the coercivity does not decrease in the sintered Nd–Fe–B/Tb–Fe–B magnets. This result verifies that the larger increase in coercivity originates from the change in anisotropy in the local region. Magnetic properties could be enhanced by tuning the interfacial chemistry.[26] In this paper, the approach to improve the coercivity is made more practical by regulating the composition and the atomic diffusion. By modifying the microstructure,[27,28] further improvement of coercivity and energy product could be anticipated in the sintered composite magnets.

4. Conclusion

In summary, the high coercivity is obtained in Nd–Fe–B/Tb–Fe–B composite magnets, and the Nd content in the Nd–Fe–B alloy is varied to regulate the element distribution. For reducing Nd content of the Nd–Fe–B alloy, the content of Tb increases in the intergranular phase, which may promote Tb substitution for Nd, thus leading to a larger increase in the anisotropy at the grain boundary. Therefore, with reducing Nd content, the coercivity, despite decreasing in the conventional Nd–Fe–B magnets, does not decrease in the sintered Nd–Fe–B/Tb–Fe–B composite magnets, and both the remanence and energy product increase. The magnetic properties in the magnets prepared by mixing Nd–Fe–B and Tb–Fe–B powders are better than those of conventional sintered (Nd,Tb)–Fe–B magnets. Further improvement of magnetic properties could be expected in sintered composite magnets by optimizing the atomic diffusion and the microstructure.

References

[1] Sagawa M, Fujimura S, Togawa N, Yamamoto H and Matsuura Y 1984 *J. Appl. Phys.* **55** 2083
[2] Sugimoto S 2011 *J. Phys. D: Appl. Phys.* **44** 064001
[3] Cai L W, Guo S, Ding G F, Chen R J, Liu J, Lee D and Yan A R 2015 *Chin. Phys. B* **24** 097505
[4] Kronmüller H, Durst K D and Sagawa M 1988 *J. Magn. Magn. Mater.* **74** 291
[5] Watanabe N, Itakura M, Kuwano N, Li D, Suzuki S and Machida K 2007 *Mater. Trans.* **48** 915
[6] Sepehri-Amin H, Ohkubo T and Hono K 2010 *J. Appl. Phys.* **107** 09A745
[7] Ma T Y, Wang X J, Liu X L, Wu C and Yan M 2015 *J. Phys. D: Appl. Phys.* **48** 215001
[8] Wang Z X, Ju J Y, Wang J Z, Yin W Z, Chen R J, Li M, Jin C X, Tang X, Lee D and Yan A 2016 *Sci. Rep.* **6** 38335
[9] Zhu M G, Li W, Wang J D, Zheng L Y, Li Y F, Zhang K, Feng H B and Liu T 2014 *IEEE Trans. Magn.* **50** 1000104
[10] Zhang X F, Lan J T, Li Z B, Liu Y L, Zhang L L, Li Y F and Zhao Q 2016 *Chin. Phys. B* **25** 057502
[11] Liu D, Zhao T Y, Li R, Zhang M, Shang R X, Xiong J F, Zhang J, Sun J R and Shen B G 2017 *AIP Adv.* **7** 056201
[12] Jin J, Ma T, Zhang Y, Bai G and Yan M 2016 *Sci. Rep.* **6** 32200

[13] Xiong J F, Shang R X, Liu Y L, Zhao X, Zuo W L, Hu F X, Sun J R, Zhao T Y, Chen R J and Shen B G 2018 *Chin. Phys. B* **27** 077504
[14] Zhang Y J, Ma T Y, Yan M, Jin J Y, Wu B, Peng B X, Liu Y S, Yue M and Liu C Y 2018 *Acta Mater.* **146** 97
[15] Wang D S, Li Z B, Liu F, Ma Q, Li Y F, Zhao Q and Zhang X F 2018 *Mater. Lett.* **228** 509
[16] Wang C G, Yue M, Zhang D T, Liu W Q and Zhang J X 2016 *J. Magn. Magn. Mater.* **404** 64
[17] Sagawa M, Fujimura S, Yamamoto H, Matsuura Y and Hiraga K 1984 *IEEE Trans. Magn.* **20** 1584
[18] Zhang L L, Li Z B, Zhang X F, Ma Q, Liu Y L, Li Y F and Zhao Q 2017 *J. Phys. D: Appl. Phys.* **50** 065001
[19] Liu J, Sepehri-Amin H, Ohkubo T, Hioki K, Hattori A, Schrefl T and Hono K 2013 *Act Mater.* **61** 5387
[20] Liu X B and Altounian Z 2012 *J. Appl. Phys.* **111** 07A701
[21] Herbst J F 1991 *Rev. Mod. Phys.* **63** 819
[22] Hu Z H, Lian F Z, Zhu M G and Li W 2008 *J. Magn. Magn. Mater.* **320** 1735
[23] Lukin A A, Kol'chugina N B, Burkhanov G S, Klyueva N E and Skotnitseva K 2013 *Inorg. Mater.: Appl. Research.* **4** 256
[24] Li H L, Li X H, Guo D F, Lou L, Li W and Zhang X Y 2016 *Nano Lett.* **16** 5631
[25] Li Z, Liu W, Zha S, Li Y, Wang Y, Zhang D, Yue M, Zhang J and Huang X 2015 *J. Magn. Magn. Mater.* **393** 551
[26] Li H L, Lou L, Hou F C, Guo D F, Li W, Li X H, Gunderov D V, Sato K and Zhang X Y 2013 *Appl. Phys. Lett.* **103** 142406
[27] Kim T H, Lee S R, Bae K H, Kim H J, Lee M W and Jang T S 2017 *Acta Mater.* **133** 200
[28] Hono K and Sepehri-Amin H 2018 *Scr. Mater.* **154** 277